

The circadian rhythm and entrainment of an internal oscillator by an external periodic signal

Nathalie Meyer and Matthias Tsai

02.12.2014

Introduction

Mammals have an internal clock called the central circadian clock that governs many behavioral and physiological parameters of the body such as sleep wake cycle, body temperature and blood pressure.

The central circadian clock is situated in the hypothalamus in the central suprachiasmatic nuclei (SCN), and has a period of approximately 24.5 hours. The signal is sent in the SCN by the retinohypothalamic tract when the entrainment force is light. The SCN sends rhythmic entrainment signals to peripheral clocks and can be modeled by an oscillator, which can be influenced by external forces such as social environment, temperature change and feeding cycles.

The model that we used is inspired by the paper “Coupling governs entrainment range of circadian clocks” (Abraham et al., 2010), which describes a study on the effect of an external entrainment force on a peripheral and internal clock. It is given by the following formula:

$$\dot{z} = (\mu + i\omega)z - z|z|^2 + F e^{i\Omega t} \quad (1)$$

μ is a parameter of the oscillator, ω is the intrinsic frequency, Ω the extrinsic frequency and F the entrainment force acting on the internal oscillator.

The goal of this study is to analyze under which conditions the oscillator of the circadian clock is synchronized with the oscillator of the external entrainment range. In a second step, the effects of a very brief time exposure of the coupling acting on the oscillator has been studied. This was simplified by assuming a very large μ .

Results:

Analysis of the non entrained model

First, F is chosen equal to zero and the model is subdivided in its cartesian coordinates using the change of variable $z = x+iy$:

$$\dot{x} = \mu x - \omega y - x^3 - xy^2 \quad (2)$$

$$\dot{y} = \mu y + \omega x - y^3 - yx^2 \quad (3)$$

In polar coordinates with $z(t) = R(t)e^{i\varphi(t)}$, the model can be rewritten as:

$$\dot{z} = \dot{R} e^{i\varphi(t)} + Ri \dot{\varphi} e^{i\varphi(t)} \quad (4)$$

$$\dot{R} = R(\mu - R^2) \quad (5)$$

$$\dot{\varphi} = \omega \quad (6)$$

Eq. (5) shows that a fixed point is located in (0,0) that must be unstable since for all $R < \sqrt{\mu}$, $\dot{R} > 0$. It also suggests a converging limit circle exists at $R = \sqrt{\mu}$, because if $R > \sqrt{\mu}$, $\dot{R} < 0$, which fulfills the last requirements for the Pointcaré Bendixon theorem postulating the necessary features for the existence of a stable limit cycle.

The isocline plot [figure 1], shows that any initial condition will converge on the stable limit circle with radius $\sqrt{\mu}$.

Analysis of the entrained model

For the case where $F \neq 0$, polar and cartesian coordinates are useful but don't get rid of the time dependence $e^{i\Omega t}$. In order to render the system time autonomous, and to set the system in a frame of reference, in which the external entrainment is static and constant, the following change of variable was applied:

$$Z(t) = z(t) e^{-i\Omega t} \quad (7)$$

Using $\Delta = \omega - \Omega$, this becomes:

$$\dot{Z} = (\mu + \Delta i)Z - Z|Z|^2 + F \quad (8)$$

This can be transformed back in cartesian coordinates of the new frame of reference:

$$\dot{X} = \mu X - \Delta Y - X(X^2 + Y^2) + F \quad (9)$$

$$\dot{Y} = \mu Y + \Delta X - Y(X^2 + Y^2) \quad (10)$$

Phase portrait of the entrained model

In order to analyze under which condition the oscillator is synchronized with the external stimulus, the phase portrait of the model was plotted for three different values of Δ and F [figure 2].

We can observe that a fixed point and a “saddle point” is seen for the case ($\Delta = 0.1, F = 0.3$), then at ($\Delta = 0.2, F = 0.6$), only the stable fixed point is seen and the last case, at ($\Delta = 0.6, F = 0.2$) an unstable fixed point is seen at the origin.

Figure [2] gives a good idea of how the fixed point are moving. To explore a bit more this move, it is useful to generate some movies of the evolution of the phase portraits while changing once Δ and once F (added in separate .gif files).

It can be observed that only the \dot{x} isocline is moving when varying F because only \dot{x} depends on the entrainment force.

Arnold Tongues and Dephasing in Phase-Locking

In order to summarize the occurrence of stable fixed point for varying Δ and F , a plot representing the stable fixed points was made in the Δ, F plane. Figure [7] shows that the stable fixed points are located within a triangle with slope $\pm F$.

Additionally, in order to investigate the effects of changing Δ on the amplitude and the relative phase of the fixed points, a plot of these dependences was computed [figure 8].

The amplitude change in a quadratic way, where as the phase has an odd function.

Maximum of amplitude is when $\Delta = 0$, and minimum is reached when $\Delta = \pm F$.

The relative phase is positively correlated with Δ and is null when $\Delta = 0$.

Order and chaos in a pulse-coupled oscillator

To study the oscillator when coupling is applied in a brief period of time, we consider a large μ which allow us to admit that only the phase dynamics matters because from Equation (5), it can be assumed that the amplitude will converge to such a big value that the external force won't significantly influence it. This allows us to analyze the following model:

$$\dot{\theta} = \omega + \sum \delta(t - nT)g(\theta(t)) \quad (9)$$

Which can be simplified by integrated over one period and adding θ_n on both side in order to get the discrete dynamical system :

$$\theta_{n+1} = \theta_n + \omega T + g(\theta_n) \quad (10)$$

Since $\theta_{n+1} = \theta_n$ at fixed points, a plot of θ_{n+1} in function of θ_n can be made for different ϵ in order to find out the values of ϵ , for which θ will converge and the system will synchronize [figure 9 and figure 10]. Fixed points can be observed for $\epsilon \in [-2.5, -1]$.

It is then possible to plot histogram of θ for varying values of ϵ between -5 and 0 [figure 11].

Several peaks of θ_{n+1} can be observed, when ϵ is smaller than -2.5 and bigger than -0.5. Between these values two peaks are observed or one if ϵ belongs to the region between -2 and -0.9.

Finally, a bifurcation diagram showing the distribution of θ_{n+1} in function of ϵ was plotted to visualize the overall analysis [figure 12].

Discussion:

Analysis of the non entrained model

Study of the non entrained model analyzes the behavior of the oscillator, when it isn't influenced by external factors. Figure [1] shows that the system always converges on a stable limit cycle of radius $\sqrt{\mu}$ surrounding an unstable stationary state located at the origin. Thus a bigger μ would result in a bigger stable limit circle.

Analysis of the entrained model

It is observed that the oscillator is synchronized with the external oscillator when the relative phase is constant. In the new frame of reference this is the case for stable fixed points of the system.

Two cases can be observed : either three fixed points (one stable, one unstable and one saddle point) or one stable fixed point. Stable fixed points seem to arise in a region where $\Delta = \pm F$. This assumption is verified in the next analysis.

Arnold Tongues and Dephasing in Phase-Locking

Figure [7], which plots the occurrence of stable fixed points in the Δ, F plane supports our hypothesis stating that stable fixed points only appear within a triangle delimited by $\Delta = \pm F$, which is defined as the Arnold tongue.

Figure [8] depicts the variation of amplitude of the fixed point for different F . The maximum of amplitude is reached when $\Delta = 0$, which make sens because it means that the difference of phase is 0 and the two oscillators are synchronized. When $\Delta = \pm F$, the amplitude is 0 which make sens because it correspond to the limit result found in Figure [7].

The variation of phase is positively correlated with Δ and passes through the origin. This makes sense because if the external factor is faster than the internal oscillator it will pull it behind and the relative phase will be negative, while if the external factor is slower, it will stabilize behind and slow the internal oscillator down.

A bigger F results into a bigger amplitude and an attenuation of the dephasing, which is due to the fact that the entrainment force will be bigger and the oscillators will synchronize closer to each other.

Order and chaos in a pulse-coupled oscillator

Figure [9] yields, for which ε values, the relative phase θ will converge and thus the systems will synchronize. When the curves cross the $\theta_{n+1} = \theta_n$ line, a fixed point can be assumed. The fixed point is stable if the absolute value of its derivative is smaller than 1 at the point where the curve crosses the $\theta_{n+1} = \theta_n$ line. This is visibly the case for $-2.5 < \varepsilon < -1$, which seems to fit the conclusions that can be made from Figure [10], where for these values of ε , θ is constrained around the point, where the respective curve crosses the $\theta_{n+1} = \theta_n$ line.

This behavior is more precisely investigated in the many histograms on Figure [11]. Especially for ε decreasing from 0 to -1, it can be observed that the relatively uniform distribution converges to a single peak phase, which describes the synchronized state of the system. When ε is further decreased, the peak first separates into two and later more peaks before reaching more chaotic distributions, in which

no synchronization can arise.

This varying dependence on the ε factor is analyzed in more details in the bifurcation diagram depicted in Figure [12]. These results correlate perfectly with the previous ones. The single peak observed in the histograms for $-2 < \varepsilon < -1$ is also visible and bifurcation behavior can be observed much more precisely. It is also possible to determine small ranges of ε , for which a synchronization takes place, that couldn't be seen on the histograms due to a too small resolution of ε (for example at $\varepsilon=-4.08$).

The ε values at the bifurcations between $\varepsilon=-2$ and $\varepsilon=-3$ are -2.098, -2.680, -2.822, -2.852 and -2.858. The first Feigenbaum constant δ can be approximated with these values and the results are 4.0986, 4.7333, 5.0000. By taking the average of these values an estimated δ of 4.6106 can be found, which is relatively close to its actual value of 4.6692 given the resolution.

Conclusion

In conclusion, synchronization of the internal oscillator and the external force occur when the difference of phase Δ is between F and $-F$. Thus synchronization is supported when F is bigger and when Δ is smaller.

Considering a non continuous entrainment range, we can say that the synchronization is obtained for ε between -2.5 and -1, where convergent states are observed. Chaos is observed for extreme values of ε (where $\varepsilon > -0.5$ or < -4.8).

If the extrinsic period is close to the intrinsic period, more order appears and chaos is decreasing.

Figures

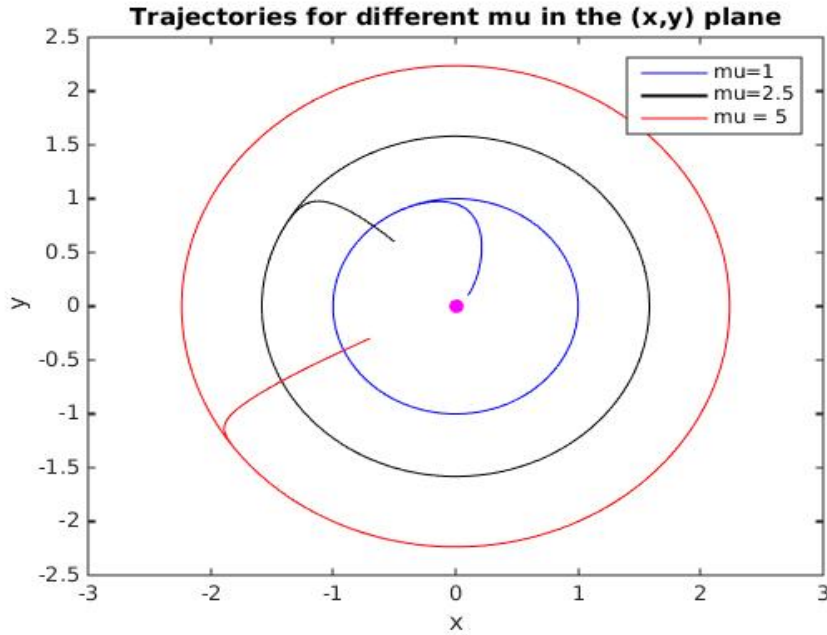


Figure 1 shows the isocline of the model without external influence, for different μ values and starting conditions. Pink dot is an unstable fixed point.

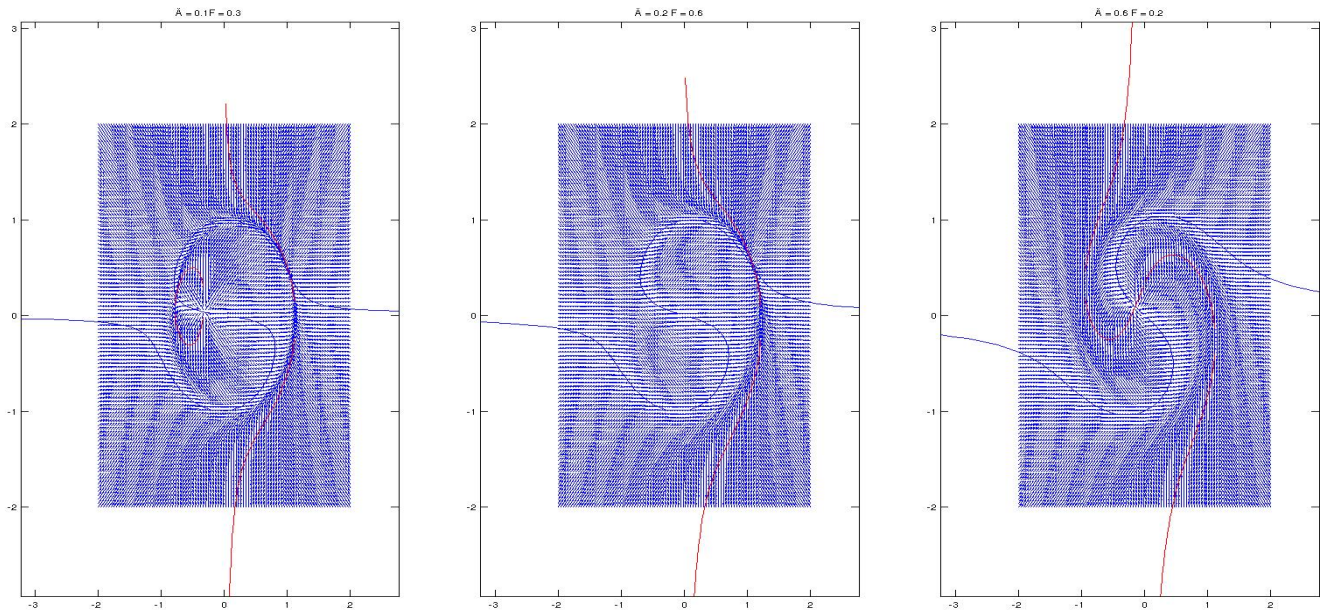


Figure 2 shows different phase portrait for different values of Δ and F : for the first picture $\Delta = 0.1$, $F = 0.3$; Three fixed points are observed one is a saddle point the other one is and the last one is an unstable fixed point. In the second picture, $\Delta = 0.2$, $F = 0.6$, only one stable fixed point is observed. The last picture, for $\Delta = 0.6$ and $F = 0.2$, shows an unstable fixed point at the origin.

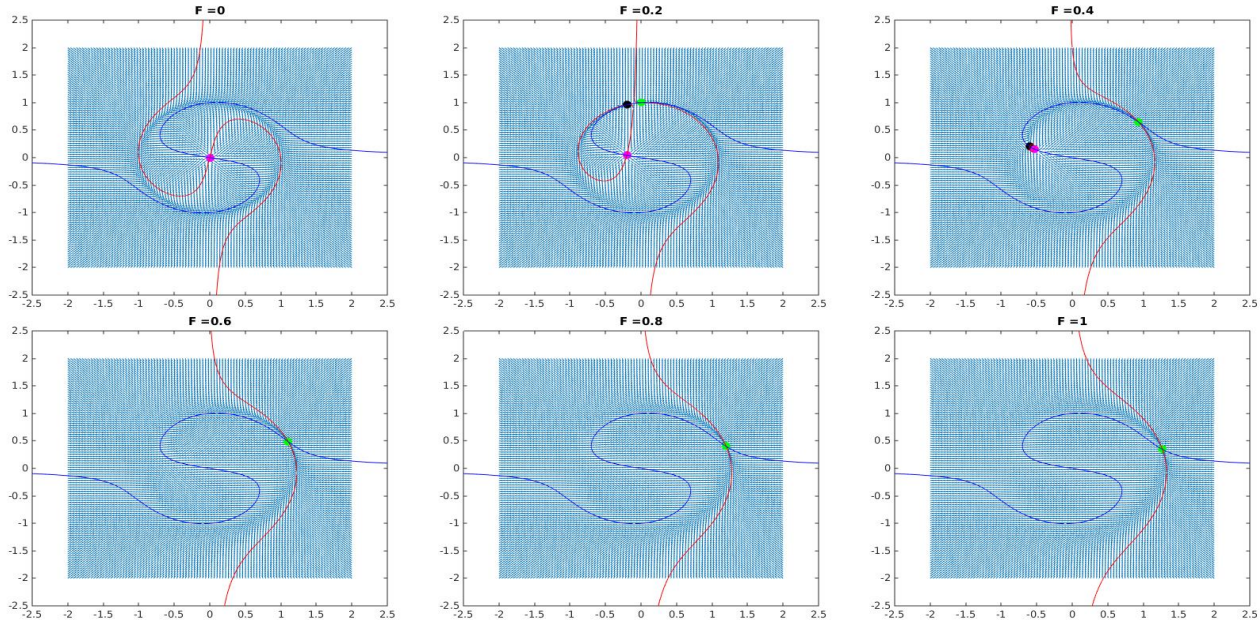


Figure 3 shows the different phase portrait of the model in the (x,y) plane when $\Delta = 0.2$, and $F \in [0, 1]$. For $F \in [0, 0.4]$ an unstable fixed point (pink dot) is observed and disappeared when $F > 0.4$. For $F \in [0.2, 1]$ a stable fixed point (green dot) is observed. There is also a saddle point (black dot) for $F \in [0.2, 0.4]$

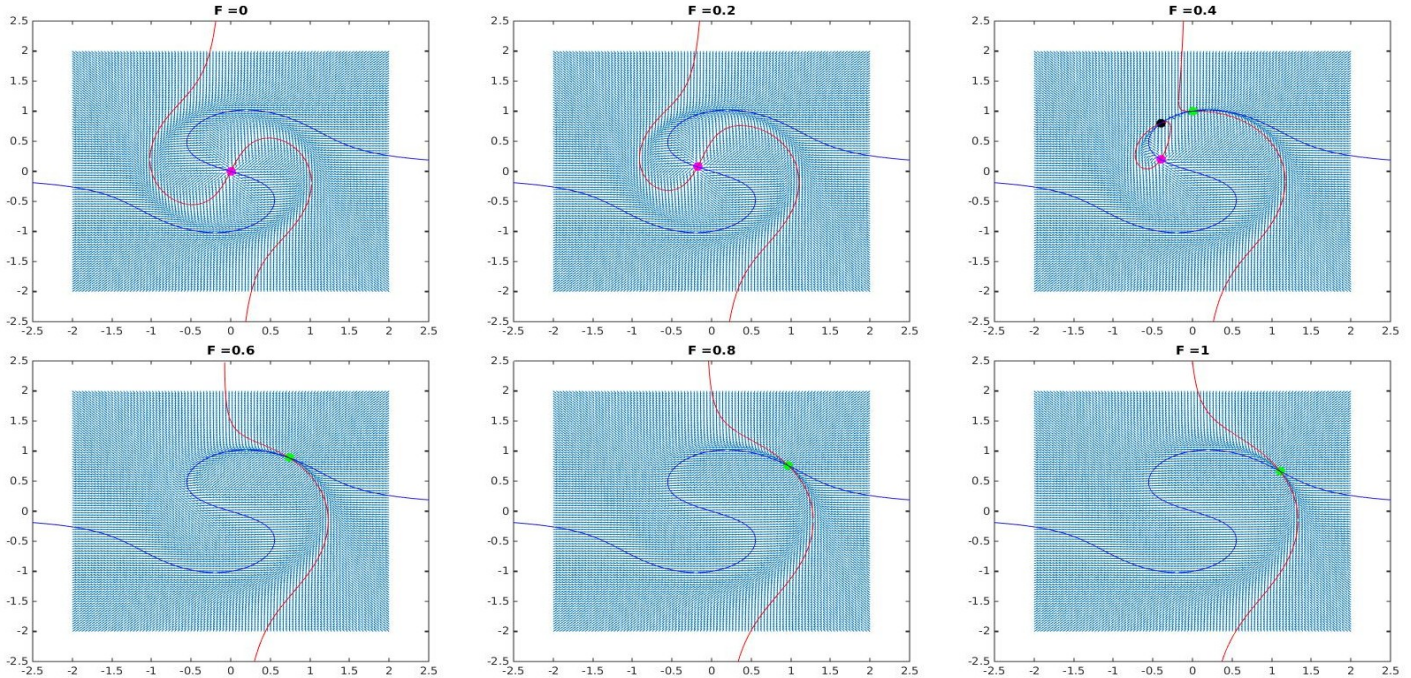


Figure 4 shows the different phase portrait of the model in the (x,y) plane when $\Delta = 0.4$, and F is varying between $[0, 1]$. For $F \in [0, 0.4]$ an unstable fixed point (pink dot) is observed and disappeared when $F > 0.4$. At $F = 0.4$ a saddle point (black dot) is visible. For $F \in [0.4, 1]$ a stable fixed point (green dot) is observed.

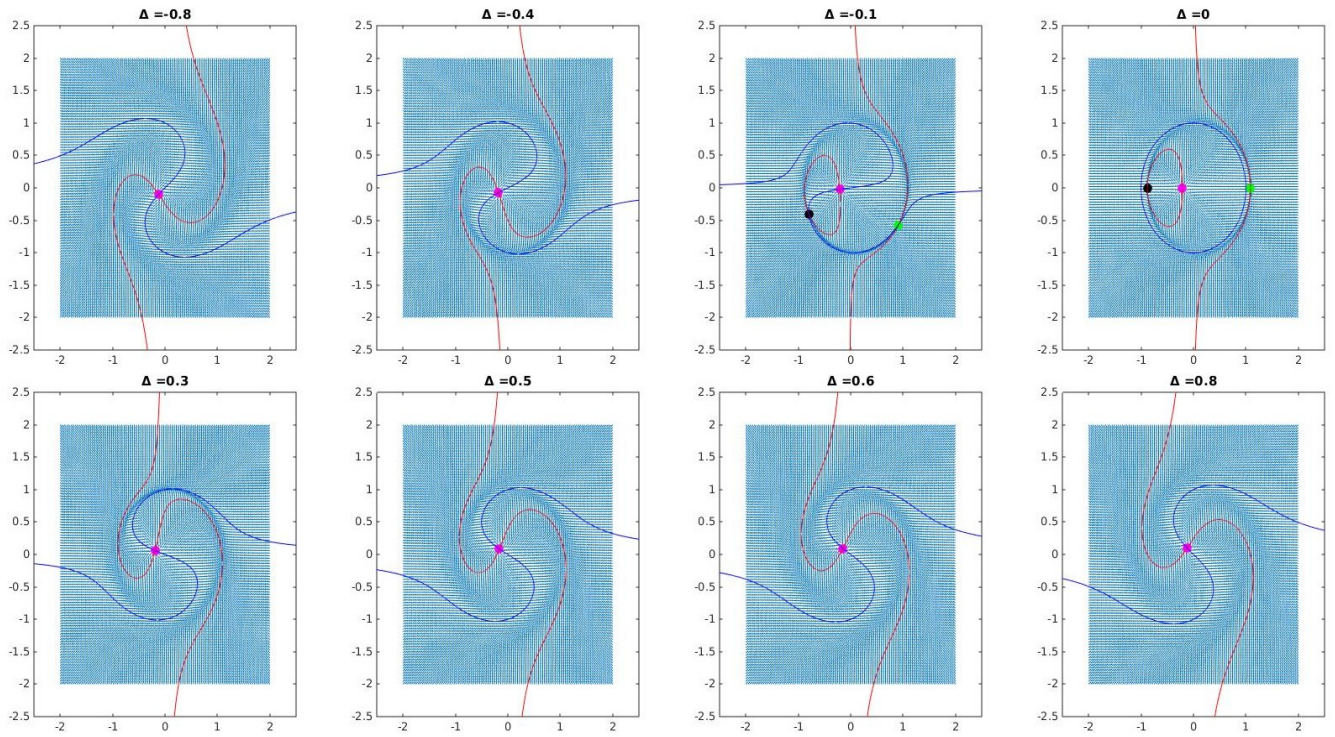


Figure 5 shows the different phase portrait of the model in the (x,y) plane when $F = 0.2$, and Δ is varying between $[-0.8, 0.8]$. one unstable fixed point (pink dot) is observed for any Δ . At $\Delta = -0.1$ and 0 , a saddle point (black dot) and a fixed point (green dot) are visible

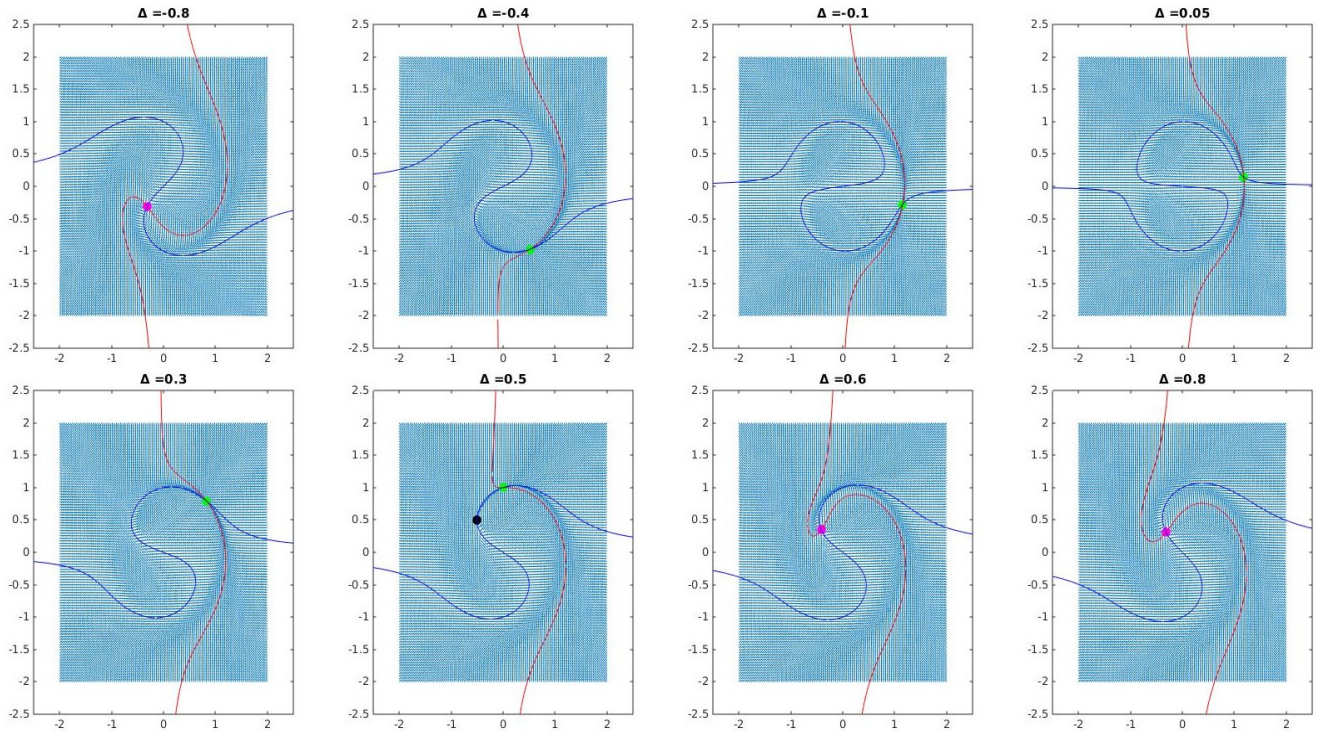


Figure 6 shows the different phase portrait of the model in the (x,y) plane when $F = 0.5$, and Δ is varying between $[-0.8, 0.8]$. One unstable fixed point (pink) is observed when $\Delta < -0.4$ and > 0.5 . between these values, a stable fixed point (green) and a saddle point (black) is observed for $\Delta = 0.5$.

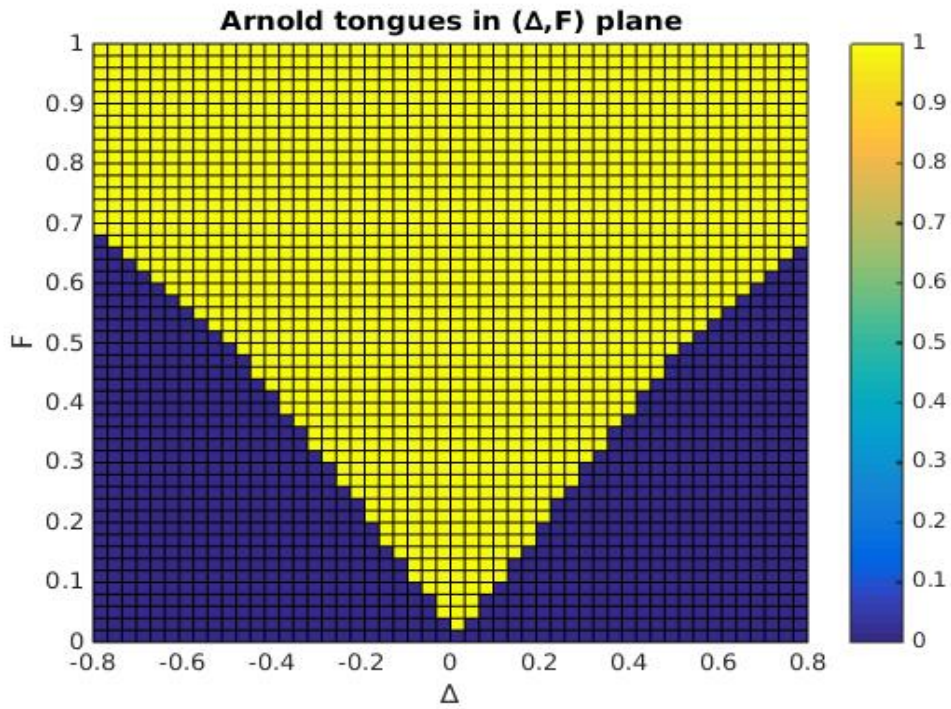


Figure 7 shows the different zone of fixed point in the plane (Δ, F) . Yellow region correspond to the stable fixed point of the system.

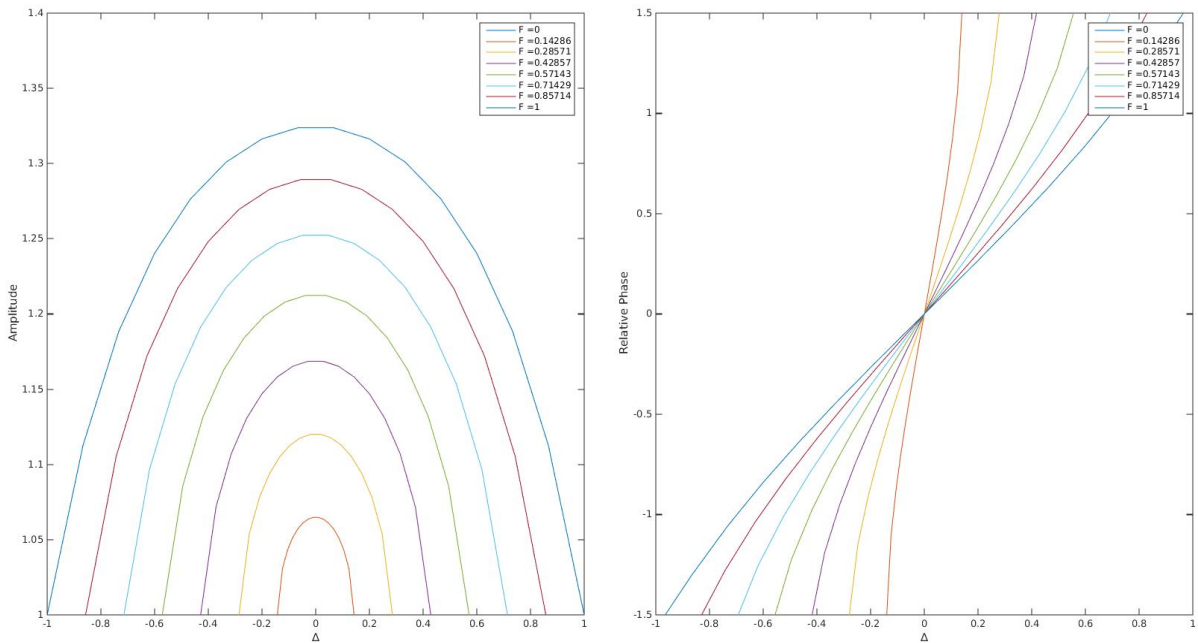


Figure 8

Left part shows how the amplitude of the oscillator is changing in function of Δ for different ε . Maximum amplitude is reached at $\Delta = 0$ and minimum is reached when $\Delta = \pm F$.

Right part shows how the phase is evaluating in function of Δ for different ε . It behaves like an odd function which is increasing when Δ is increasing and is 0 when Δ is 0.

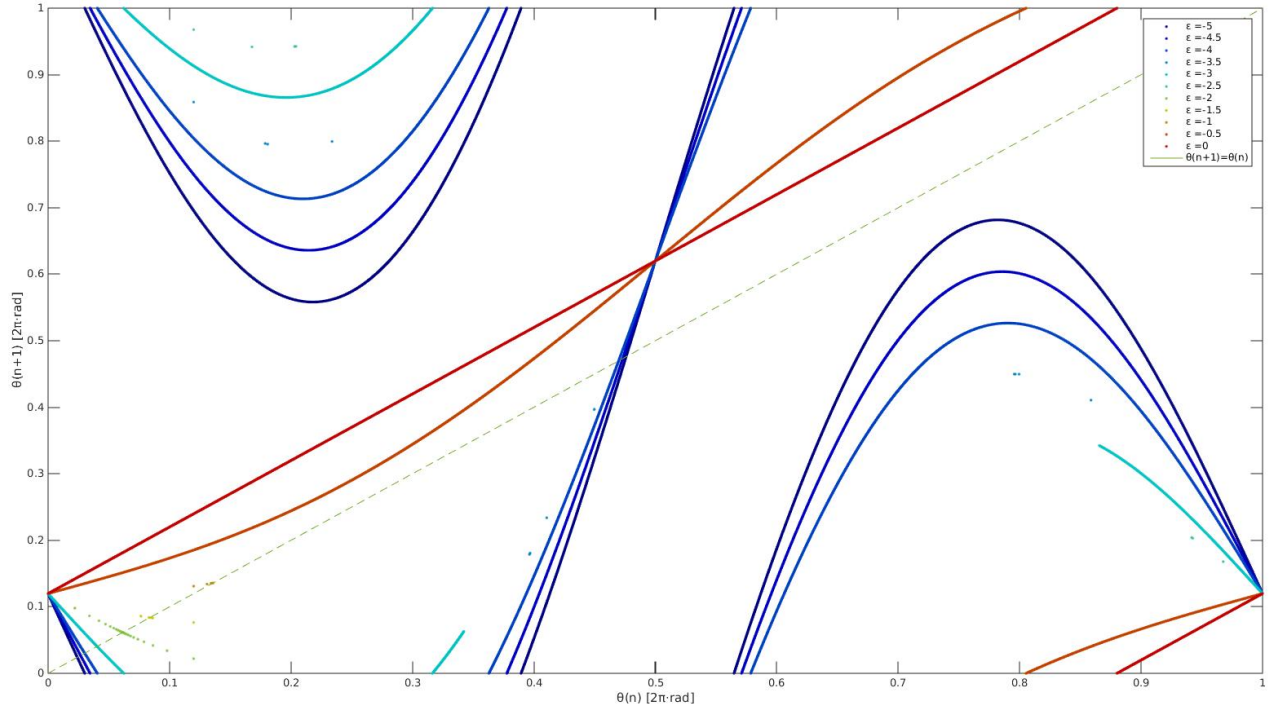


Figure 9 : Plot of the computed θ_{n+1} in function of θ_n for different ϵ . fixed point are seen when $\theta_{n+1} = \theta_n$. Stable fixed points are observed for $\epsilon > -3.5$ and < -2.5 .

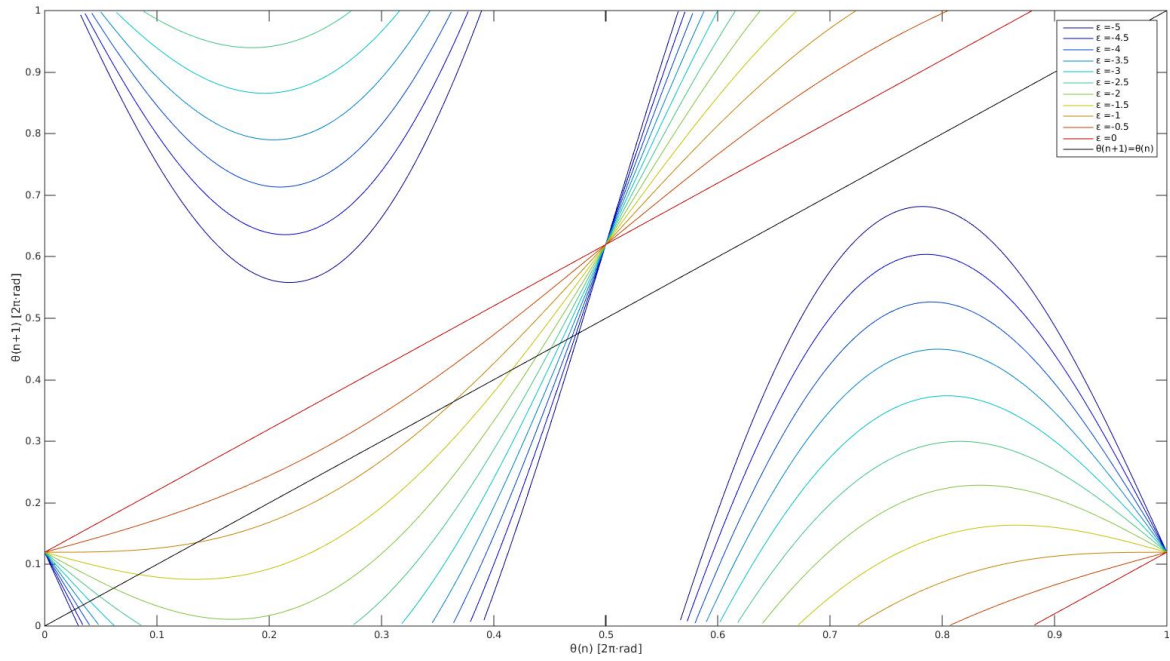


Figure 10 : Plot of θ_{n+1} in function of a range of θ_n for different ϵ . Fixed point are seen when $\theta_{n+1} = \theta_n$ and therefore for every $\epsilon < -1$.

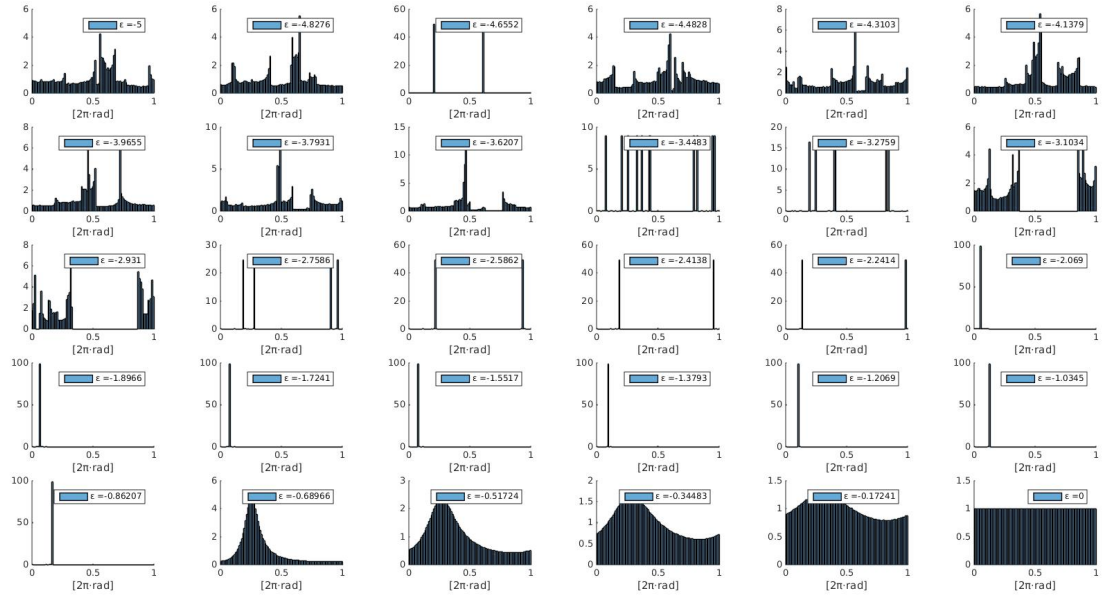


Figure 11

Histogram of θ_n for different values of ϵ . For ϵ between -2.5 and -1 single peaks are observed and the states are ordered. For ϵ with more homogeneous distribution, the state is more chaotic.

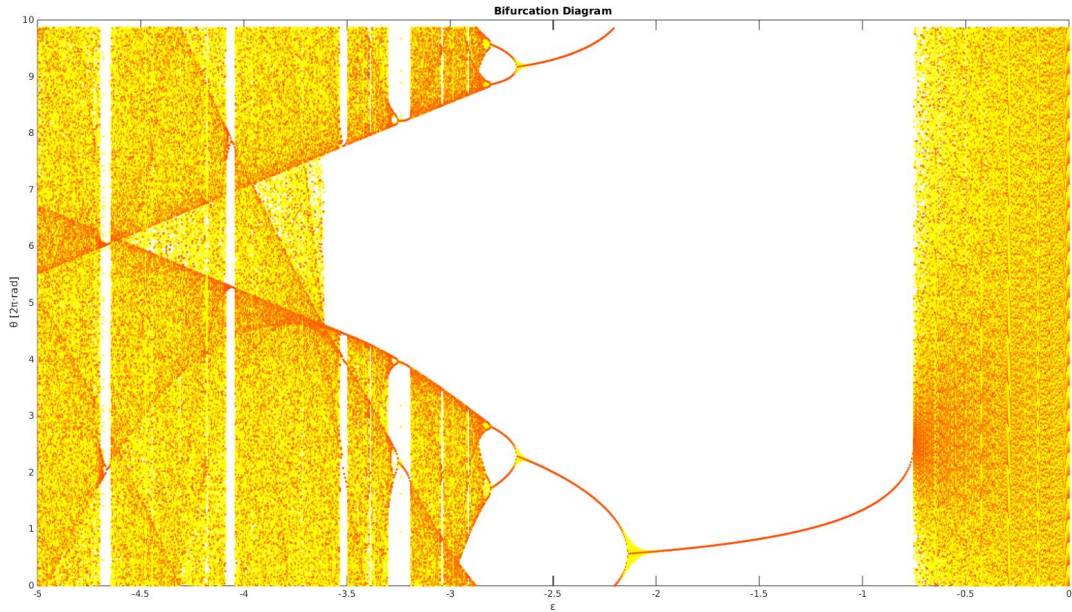


Figure 12

Bifurcation diagram of θ_n in function of ϵ . Chaos is observed for values of ϵ smaller than -3.5 and bigger than -0.5 and in general if the complete y axis is filled. Fixed point and bifurcation state are observed for ϵ between -2.5 and -1 and in general when a thin line is observed.

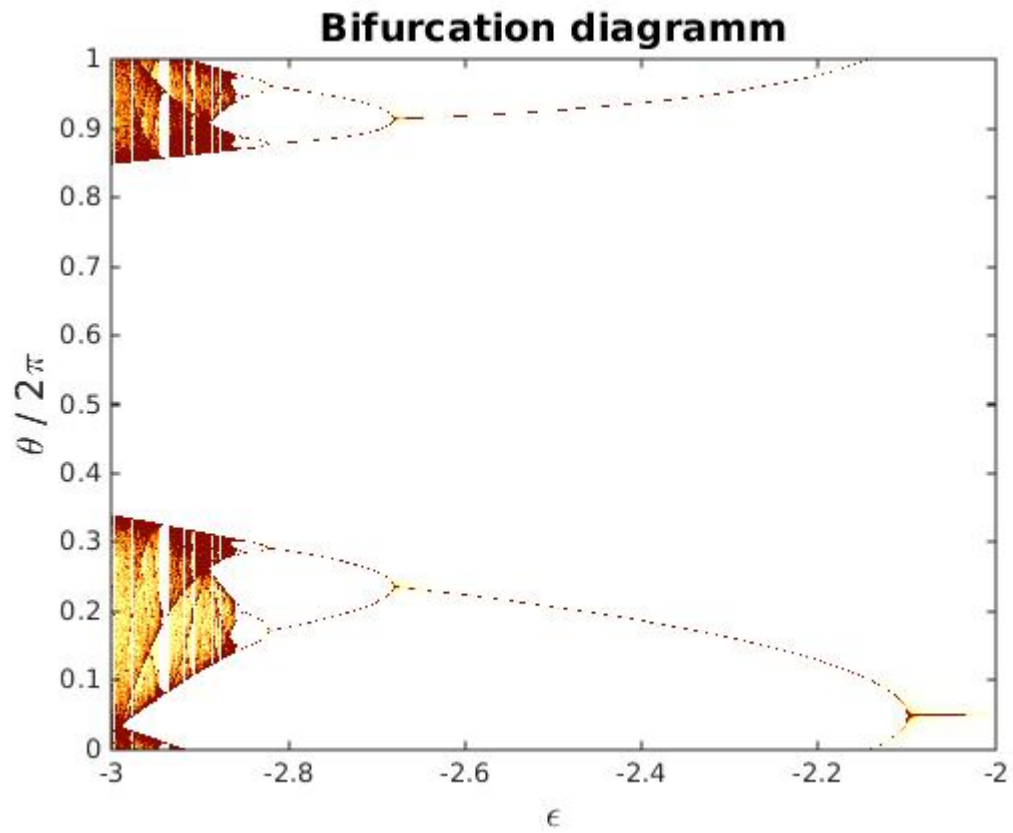


Figure 13 Zoom on the bifurcation phase of the bifurcation diagram. Bifurcation points are seen for ϵ equal to -2.098, -2.680, -2.822, -2.852 and -2.858.